



## Future regional Arctic sea ice declines

James E. Overland<sup>1</sup> and Muyin Wang<sup>2</sup>

Received 25 May 2007; revised 19 July 2007; accepted 8 August 2007; published 8 September 2007.

[1] Because animals and humans respond to seasonally and regionally varying climates, it is instructive to assess how much confidence we can have in regional projections of sea ice from the 20 models provided through the International Panel on Climate Change Fourth Assessment Report (AR4) process (IPCC 2007). Based on the selection of a subset models that closely simulate observed regional ice concentrations for 1979–1999, we find considerable evidence for loss of sea ice area of greater than 40% by 2050 in summer for the marginal seas of the Arctic basin. This conclusion is supported by consistency in the selection of the same models across different regions, and the importance of thinning ice and increased open water at mid-century to the rate of ice loss. With less confidence, we find that the Bering, Okhotsk and Barents Seas have a similar 40% loss of sea ice area by 2050 in winter. Baffin Bay/Labrador shows little change compared to current conditions. These seasonal ice zones have large interannual/decadal variability in addition to trends. Large model-to-model differences were seen for the Kara/Laptev Seas and East Greenland. With a careful evaluation process, AR4 sea ice projections have some utility for use in assessing potential impacts over large Arctic subregions for a 2020–2050 time horizon. **Citation:** Overland, J. E., and M. Wang (2007), Future regional Arctic sea ice declines, *Geophys. Res. Lett.*, 34, L17705, doi:10.1029/2007GL030808.

### 1. Introduction

[2] Annual average, Arctic-mean climate projections are useful for change detection purposes, but seasonally and regionally varying climate estimates have more direct associations and impacts on humans and other ecosystem components. Thus it is instructive to assess how much confidence we can have in regional climate projections. Loss of ice has major impacts on marine ecosystems, transportation, and feedbacks to the larger climate system. Projections of summer Arctic-wide sea ice extent by 2100 from the IPCC-AR4 models are for losses of 50 to 80% depending on the emission scenarios, with large model-to-model differences [Zhang and Walsh, 2006; Arzel et al., 2006]. The prospect of major summer sea ice losses at mid-century [Holland et al., 2006] is a rather startling result from several of the AR4 models, relative to earlier model estimates of ice loss toward the end of the century. Here we examine the regional variation in sea ice loss in

the Arctic basin for summer (August–September) and the more southerly seasonal ice zones (SIZ) for winter (March–April).

[3] The AR4 sea ice simulations for the 20th century show a considerable range of values when compared to observations [Stroeve et al., 2007]. Our experience [Overland and Wang, 2007] as well as others [Knutti et al., 2006] suggest that one method to increase confidence in climate projections is to constrain the number of models by removal of major outliers through validating historical simulations against observations. This requirement is especially important for the Arctic, as the rate of loss of 21st century sea ice in the models is correlated to the magnitude of the initial conditions at the end of the 20th century [Zhang and Walsh, 2006; Arzel et al., 2006]. On the other hand we need to retain a robust number of models (at least 5–10) as a method to sample model parameterization uncertainty and other model differences, as no single model approaches perfection.

[4] We consider AR4 model projections out to 2050, based on a middle range greenhouse emissions scenario, A1B, from the Special Report on Emission Scenarios (SRES). Because of the lag response of climate to CO<sub>2</sub>, much of the impact at 2050 depends on an emission scenario based on reasonable extrapolation of current conditions over the next few decades, rather than largely

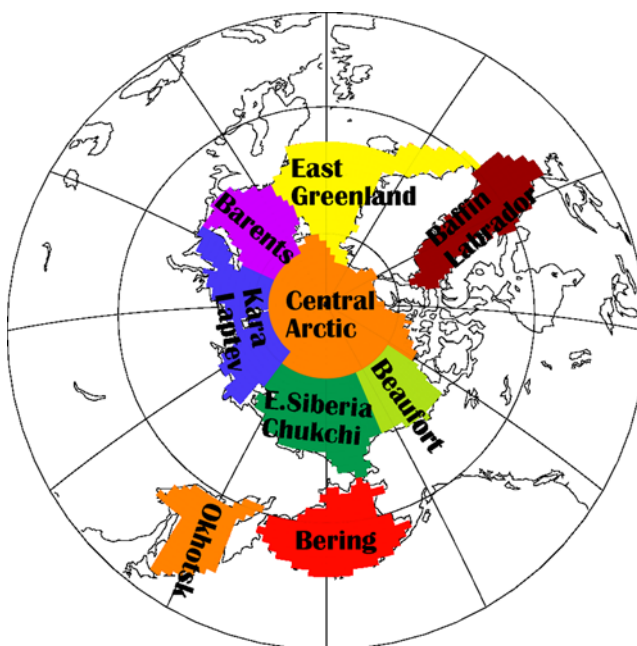


**Figure 1.** Area mask of Arctic basin marginal seas and seasonal ice zones.

<sup>1</sup>Pacific Marine Environmental Laboratory, NOAA, Seattle, Washington, USA.

<sup>2</sup>Joint Institute for the Study of the Atmosphere and Ocean, University of Washington, Seattle, Washington, USA.

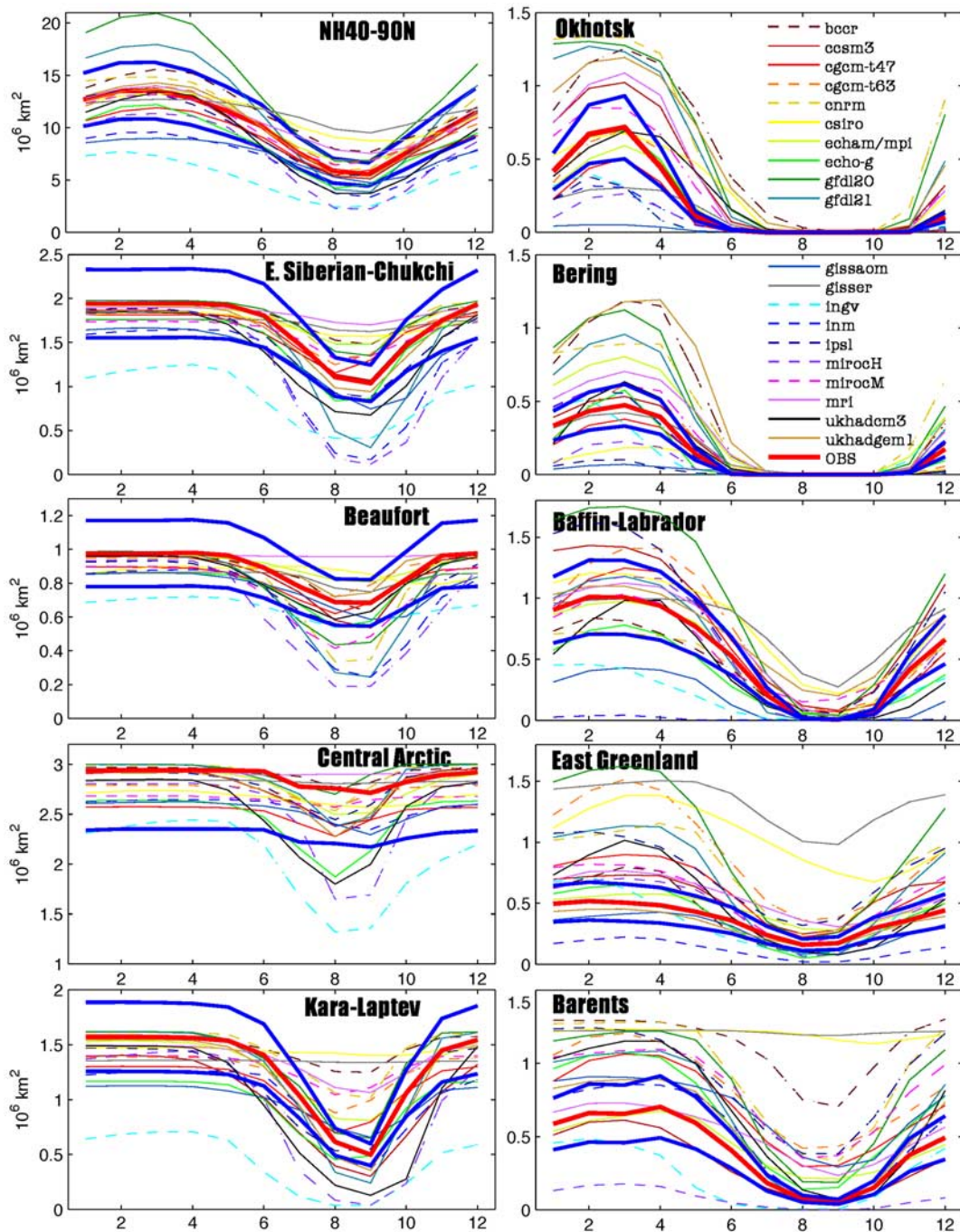


**Figure 2.** Seasonal cycle of ice area simulated by each model (colored thin lines) and observations (thick red line) for each region, averaged for 1979–1999. The thick blue lines indicate the limits of the selection rule for the Arctic basin (20%, left plots) and SIZ (30%, right plots). Solid lines indicate models with more than one ensemble are provided by the models, while the dashed lines are the single ensemble from that model.

uncertain social and technology forecasts for the end of the century [Chapman and Walsh, 2007]. Use of this 2050 horizon as an outer limit for projections is substantiated by the small differences between the impacts from different SRES scenarios for the first half of the 21st century (Figure SPM-5, Intergovernmental Panel on Climate Change, 2007, Working Group 1 Report, <http://www.ipcc.ch/>). For

the near term out to 2020, one might expect greenhouse impacts to only begin to emerge from the known large decadal variability in the Arctic; such variability is due to atmosphere heat advection [Overland and Wang, 2005; Serreze and Francis, 2006; Maslanik et al., 2007], ocean heat advection [Bitz et al., 2006; Shimada et al., 2006], and local radiative processes [Ikeda et al., 2003; Francis et al., 2005].

**Table 1.** List of Models<sup>a</sup>

| Model Number | Model Name       | NH 40–90N | Kara - Laptev | E Siberia-Chukchi | Beaufort | Central Arctic | East Greenland | Okhotsk | Bering | Baffin - Labrador | Barents | Sum            |
|--------------|------------------|-----------|---------------|-------------------|----------|----------------|----------------|---------|--------|-------------------|---------|----------------|
| 1            | bccr-BCM         |           |               |                   | X        | X              |                |         |        | X                 |         | 3              |
| <b>2</b>     | <b>ccsm3</b>     | X         |               | X                 | X        | X              |                |         | X      |                   | X       | 6              |
| <b>3</b>     | <b>cgcm-t47</b>  | X         | X             | X                 | X        | X              |                | X       | X      | X                 |         | 8              |
| <b>4</b>     | <b>cgcm-t63</b>  | X         |               | X                 | X        | X              |                | X       | X      |                   |         | 6              |
| 5            | cnrm             | X         |               |                   |          | X              |                |         |        | X                 |         | 3              |
| 6            | csiro-MK3.0      |           |               |                   |          | X              |                | X       |        | X                 |         | 3              |
| 7            | echam5/mpi       | X         |               |                   | X        | X              | X              | X       |        | X                 | X       | 7              |
| 8            | echo-g           | X         | X             | X                 | X        |                | X              | X       | X      | X                 |         | 8              |
| 9            | gfdl20           | X         | X             |                   |          | X              |                |         |        |                   |         | 3              |
| 10           | gfdl21           |           |               |                   |          | X              |                |         |        | X                 |         | 2              |
| <b>11</b>    | <b>gissaom</b>   | X         |               | X                 | X        | X              | X              |         |        |                   | X       | 6              |
| 12           | gisser           |           |               |                   | O        | O              |                |         | O      | O                 |         | 0 <sup>b</sup> |
| 13           | ingv             |           |               |                   | X        |                | X              |         | X      |                   | X       | 4              |
| 14           | inm              |           |               |                   |          | X              |                |         | X      |                   | X       | 3              |
| <b>15</b>    | <b>ipsl</b>      | X         | X             | X                 | X        | X              |                |         |        |                   |         | 5              |
| 16           | mirocH           |           |               |                   |          |                |                |         |        | X                 |         | 1              |
| 17           | mirocM           | X         |               | X                 |          | X              |                | X       | X      | X                 |         | 6              |
| 18           | mri              |           |               |                   |          | X              |                |         |        | X                 | X       | 3              |
| 19           | ukhadcm3         |           |               |                   | X        |                |                | X       |        | X                 |         | 3              |
| <b>20</b>    | <b>ukhadgem1</b> | X         |               | X                 | X        | X              | X              |         |        | X                 | X       | 7              |
| Total        |                  | 11        | 4             | 8                 | 11       | 15             | 5              | 7       | 7      | 12                | 7       |                |

<sup>a</sup>X indicates passing outlier screening. Bold indicates common performance for the Arctic basin.

<sup>b</sup>The GISS-ER model has little seasonal variation (Figure 2) and is excluded from statistics and future projections, indicated by “O.”

[5] In the next section we investigate model selection relative to 1979–1999 ice conditions. This is followed by a discussion of 21st century projections.

## 2. Annual Cycle of Sea Ice in Nine Regions

[6] For the loss of sea ice at the end of summer (August or September), we divide the Arctic basin into sectors: the Beaufort Sea, East Siberian-Chukchi Seas, Kara-Laptev Seas, central Arctic (north of 80°N), and the total Arctic ice cover-NH (Figure 1). For the winter maxima of the SIZ (March or April), we include the Barents, Okhotsk, and Bering Seas, East Greenland, and Baffin Bay/Labrador. Sea ice area for 1979–1999 is calculated from the Hadley Center analysis of ice fraction (HadISST) [Rayner *et al.*, 2003]. There could be some concern about using area instead of extent for the summer conditions based on the use of passive microwave data in HadISST. We have completed the analysis using both area and extent, with only minor differences in model selection. Further, we compared HadISST to the National Ice Center sea ice analyses in September, and find small differences at the grid resolution and multiyear average of our analysis.

[7] Figure 2 shows the model simulated annual cycle of sea ice area based on concentration for these 9 regions and total summer Arctic (NH) from the twenty AR4 models listed in Table 1 ([http://www-pcmdi.llnl.gov/ipcc/about\\_ipcc.php](http://www-pcmdi.llnl.gov/ipcc/about_ipcc.php)). The model simulated ice areas for the Beaufort Sea have a smaller range than for the Siberian side. All Arctic basin regions suggest several model outliers relative to observations (thick red line on all plots). The relative spread of model results for the SIZ is greater than for the Arctic basin. Many models for East Greenland and Barents have too much ice in winter. The overestimation of ice in the Barents is consistent with the hypothesis that ocean heat transport is

underestimated in many models [Parkinson *et al.*, 2006]. East Greenland is an advective region of ice drift which could lead to large uncertainties. The Bering Sea, Sea of Okhotsk and Baffin Bay/Labrador have several models that cluster near the observations, but also have outliers.

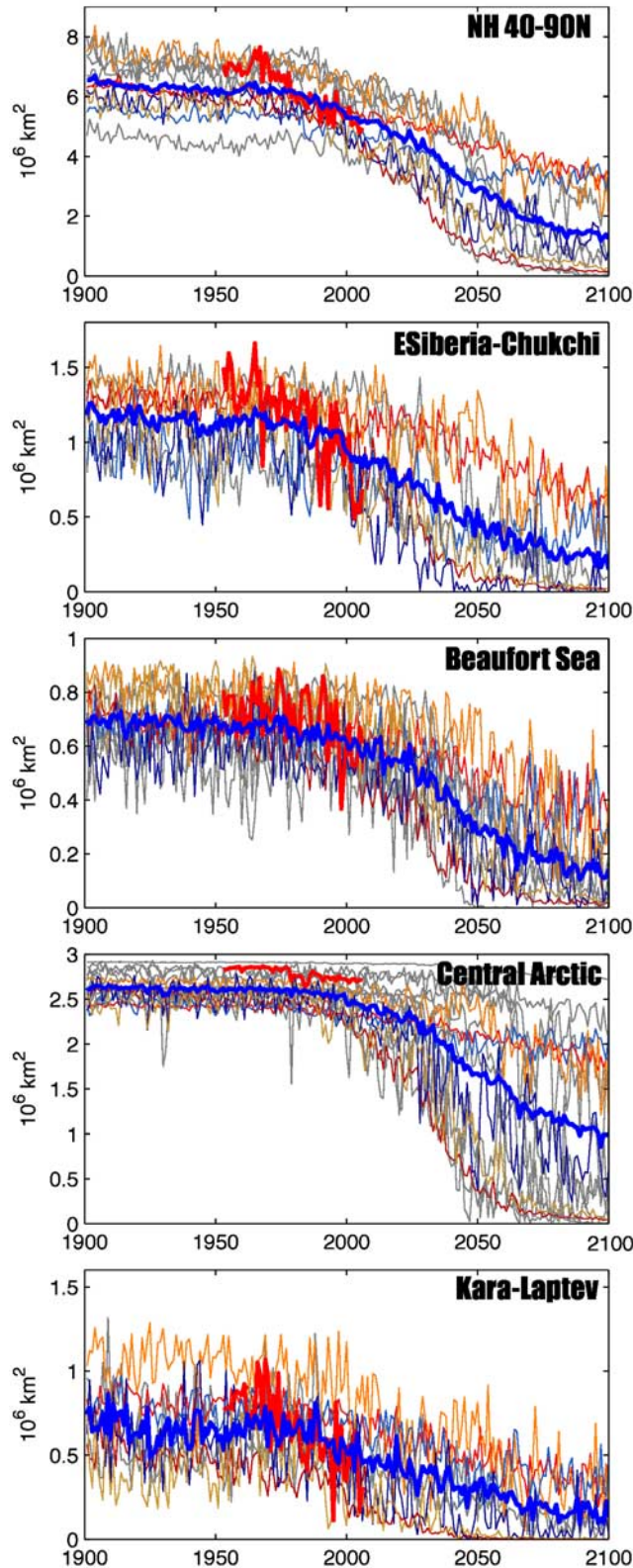
[8] Our purpose is not to select the “best” models, but to insure that the initial conditions at the end of the 20th century are reasonable before considering 21st century projections. For the summer Arctic basin regions, a limit of within 20% of the observed ice area for 1979–1999 (thick blue lines in Figure 2) is applied to all models, similar to Stroeve *et al.* [2007]. For the SIZ, with smaller baseline areas, we relaxed this limit to within 30%. We also drop the GISS-ER model (#12) for its lack of a seasonal cycle. Out of 20 potential models, 11 are retained for the Arctic wide area, 4, 8 and 11 are retained for the three marginal seas: Kara/Laptev, East Siberian/Chukchi, and Beaufort Seas, and 15 models are retained for the central Arctic. If we drop the Kara/Laptev Sea as having large uncertainties, six common models (#2, 3, 4, 11, 15 and 20) are retained for all the regions in summer (Table 1, bold letters). For the winter SIZ the number of outliers is large and their distributions are not always symmetric about the observation value. We retain 7 models each for the Bering, Okhotsk, and Barents Seas, 12 for Baffin Bay and 5 for East Greenland.

## 3. Projected Sea Ice Area

### 3.1. Arctic Basin Summer

[9] The simulated summer (August and September average) Arctic-wide sea ice area for the 20th century and projected area during the 21st century is shown at the top left of Figure 3 from 11 retained models. As noted in the introduction, several models that start with too much ice in the late 20th century, end up with more ice in their

21st century projections; a similar effect is reported by *Stroeve et al.* [2007]. The marginal seas of the Arctic basin show an increased rate of ice loss in the mid 21st century relative to the 20th century. In Figure 4 summary results



show the relative amount of ice area remaining in 2045–2054 relative to 1979–1999 based on individual model ensemble averages. Ensemble and time averaging suppresses natural variability relative to the forced trends. By 2050, 7 of 11 models estimate a loss of 40% or greater of summer Arctic ice area. Six of 8 models show a greater than 40% ice loss in the East Siberian/Chukchi Seas and 7 of 11 models show this loss for the Beaufort Sea. The percentage of models with major ice loss could be considered higher, as two of the models that retain sea ice are from the same Canadian source and thus, while they have different grid resolutions, cannot be considered to be completely independent. These results present a consistent picture: there is a substantial loss of sea ice for most models and regions by 2050. As noted above, six common models were selected for all of the summertime regions based on late 20th century evaluations. The central Arctic (Figure 4, lower left) shows a bimodal distribution of ice remaining in 2050; for some models there is a substantial ice reduction, while for other there remains a sanctuary region (Figure 3). The CCSM3 model [Holland *et al.*, 2006] is one of the models with the most rapid ice loss in the 21st century. Further confidence is provided through understanding of the physical causes of ice loss in the models. Other authors [Holland *et al.*, 2006; Winton, 2006] discuss that the main physical process simulated in the models is an accelerated increase of open water by 2050, based on thinning ice and ice albedo feedback in response to increasing greenhouse emissions. This is not to say that more complicated climate processes will not also play a role in the real world during the 21st century.

### 3.2. Seasonal Ice Zones

[10] Time series for sea ice in the SIZ during winter (March and April average) are shown in Figure 5. Except for East Greenland which is represented by too few models, there is substantial interannual and decadal variability in all SIZs model projections (gray lines), which vary around the model mean trends (blue) during the 21st century. By 2050, 5 of 7 models show 40% or more ice loss in the Bering and Barents Seas and 4 of 7 models for the Okhotsk Sea (Figure 4, right). According to these models, Baffin Bay does not show significant ice loss by 2050. This is consistent with a lack of a 21st century temperature trend southwest of Greenland in the IPCC models [Chapman and Walsh, 2007]. Different models were selected in different SIZ regions. This may be due to their geographic separation or

**Figure 3.** Summer (August and September average) sea ice area simulated/projected by models for 1900–2100 from the models that pass 20% criterion. The six models which qualified for all of the four regions (NH, E. Siberian-Chukchi, Beaufort, and central Arctic) are in color. Other models are shown in gray. The number of models is different for each region; see Table 1 for the list of the models. Thick blue line is the multi-model ensemble mean. Thick red line is based on observations (HadISST). For the Kara-Laptev we show additional results from the set of six models mentioned above.

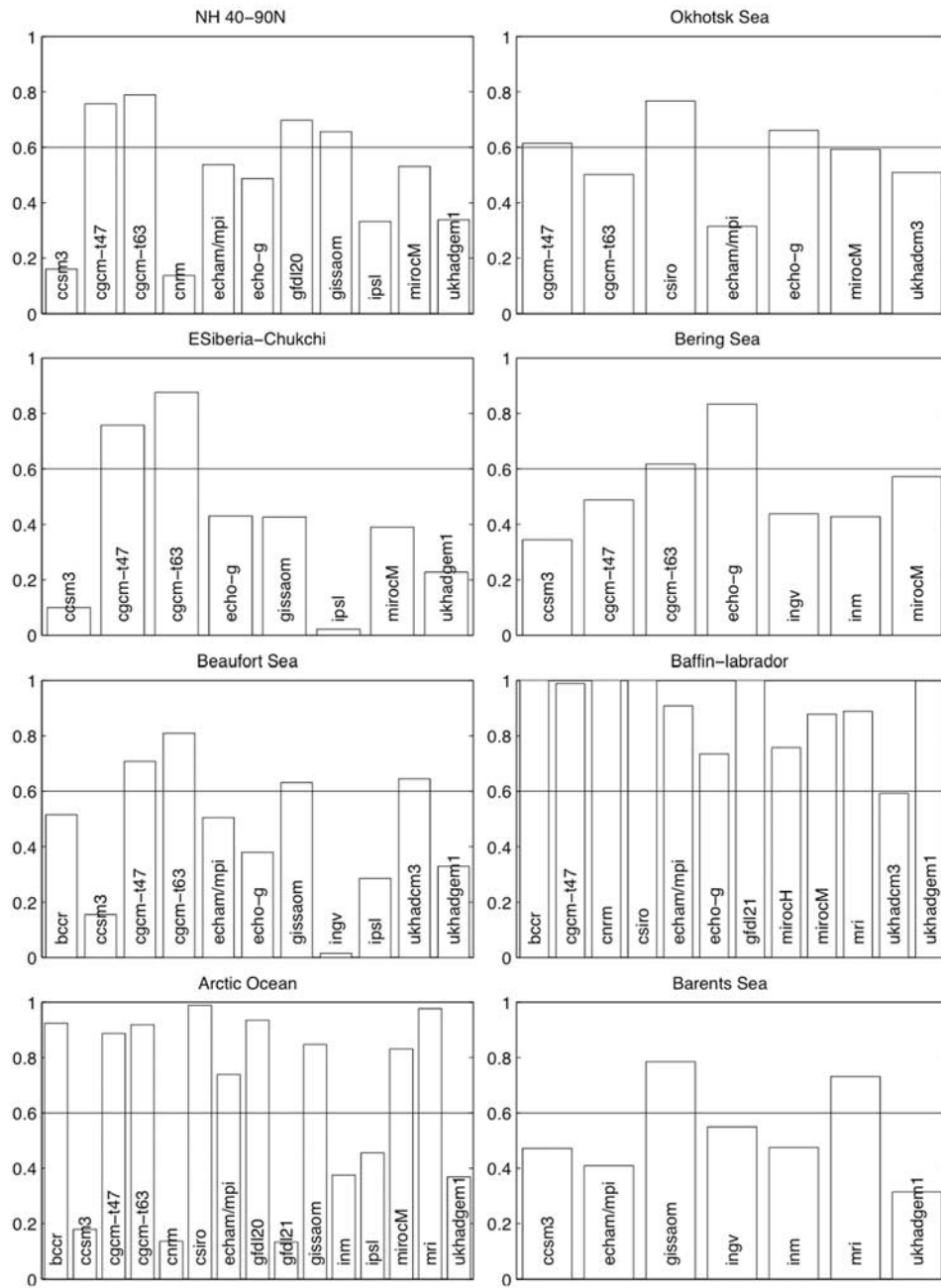


**Figure 4.** Change of ice area between 2045–2054 and 1979–99 given as a fraction of ice are remaining for regions in (left) summer and (right) winter. The models that passed the selection criteria are shown. The line in each plot indicates a 40% ice area reduction at 2050.

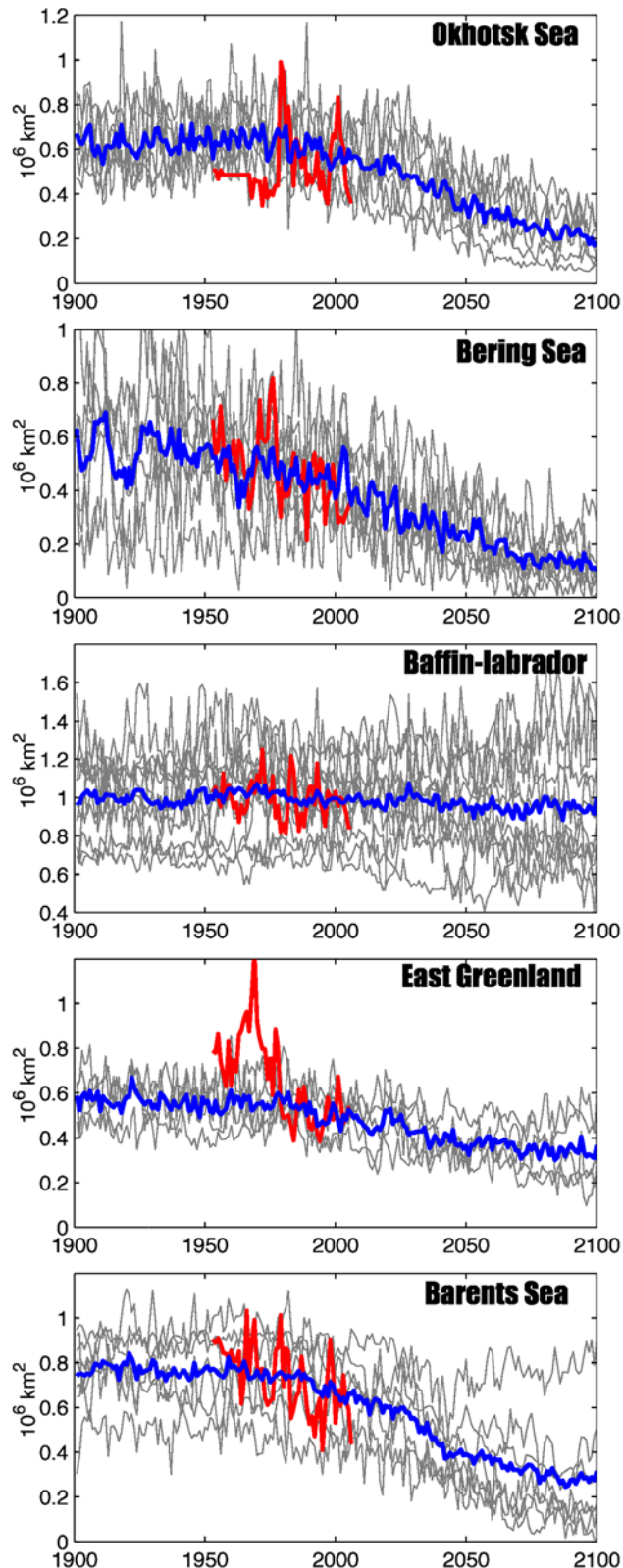


**Figure 5.** Winter (March and April average) sea ice area for seasonal ice zones (SIZ) as simulated/projected by models for 1900–2100. Different models are selected for each region as shown in Table 1, and are shown by grey lines. The thick blue line indicates the multi-model ensemble mean. The thick red line is based on observations (HadISST).

that different processes which control sea ice area may be active, such as ocean advection or polynya formation.

#### 4. Conclusion

[11] Starting from a collection of 20 models from the IPCC AR4, we pre-screened subsets of models to remove potential outliers based on comparison to late 20th century observations. These subsets show a consistent loss of greater than 40% in sea ice area by 2050 for the total area and for most Arctic basin marginal seas in summer as well as the SIZs in winter, except for the Baffin Bay region which shows no loss. For the Arctic basin this conclusion is supported by a common selection of six models across regions and by other authors who note an increased importance of thin ice and open water/ice albedo feedback. Large model-to-model variability was shown for the Kara/Laptev Seas and East Greenland. SIZs show considerable future interannual and decadal variability in addition to trends. With a careful evaluation process, IPCC AR4 sea ice projections have some utility for large Arctic subregions with regards to transportation and ecological impacts.

[12] **Acknowledgments.** We would like to thank the NOAA Arctic Program and the NSF sponsored North Pole Environmental Observatory Project for their support. We thank Xiangdong Zhang for sharing his sub-arctic sea mask design and Sigrid Salo for working with the National Ice Center ice analyses. We acknowledge the modeling groups for making their model output available as part of the World Climate Research Programme's CMIP3 multi-model dataset, the Program for Climate Model Diagnosis and Intercomparison for collecting and archiving this data, and the WCRP's Working Group on Coupled Modeling for organizing the model data analysis activity. The WCRP CMIP3 multi-model data set is supported by the U.S. Department of Energy Office of Science. This publication is partially funded by the Joint Institute for the Study of the Atmosphere and Ocean (JISAO) under NOAA Cooperative Agreement NA17RJ1232, contribution 1412. PMEL contribution 3081.

#### References

- Arzel, O., T. Fichefet, and H. Goosse (2006), Sea ice evolution over the 20th and 21st centuries as simulated by current AOGCMs, *Ocean Modell.*, *12*, 401–415.
- Bitz, C. M., et al. (2006), The influence of sea ice on ocean heat uptake in response to increasing CO<sub>2</sub>, *J. Clim.*, *19*, 2437–2450.
- Chapman, W. L., and J. E. Walsh (2007), Simulations of Arctic temperature and pressure by global coupled models, *J. Clim.*, *20*, 609–632.
- Francis, J. A., E. Hunter, J. R. Key, and X. Wang (2005), Clues to variability in Arctic minimum sea ice extent, *Geophys. Res. Lett.*, *32*, L21501, doi:10.1029/2005GL024376.
- Holland, M. M., C. M. Bitz, and B. Tremblay (2006), Future abrupt reductions in the summer Arctic sea ice, *Geophys. Res. Lett.*, *33*, L23503, doi:10.1029/2006GL028024.
- Ikeda, M., J. Wang, and A. Makshtas (2003), Importance of clouds to the decaying trend and decadal variability in the Arctic ice cover, *J. Meteorol. Soc. Jpn.*, *81*, 179–189.
- Knutti, R., G. Meehl, M. R. Allen, and D. A. Stainforth (2006), Constraining climate sensitivity from the seasonal cycle in surface temperature, *J. Clim.*, *19*, 4224–4233.
- Maslanik, J., S. Drobot, C. Fowler, W. Emery, and R. Barry (2007), On the Arctic climate paradox and the continuing role of atmospheric circulation in affecting sea ice conditions, *Geophys. Res. Lett.*, *34*, L03711, doi:10.1029/2006GL028269.
- Overland, J. E., and M. Wang (2005), The third Arctic climate pattern: 1930s and early 2000s, *Geophys. Res. Lett.*, *32*, L23808, doi:10.1029/2005GL024254.
- Overland, J. E., and M. Wang (2007), Future climate of the North Pacific Ocean, *Eos Trans. AGU*, *88*(16), 178, 182.
- Parkinson, C. L., K. Y. Vinnikov, and D. J. Cavalieri (2006), Evaluation of the simulation of annual cycle of Arctic and Antarctic sea ice coverages by 11 major global climate models, *J. Geophys. Res.*, *111*, C07012, doi:10.1029/2005JC003408.
- Rayner, N. A., D. E. Parker, E. B. Horton, C. K. Folland, L. V. Alexander, D. P. Rowell, E. C. Kent, and A. Kaplan (2003), Global analyses of sea

- surface temperature, sea ice, and night marine air temperature since the late nineteenth century, *J. Geophys. Res.*, *108*(D14), 4407, doi:10.1029/2002JD002670.
- Serreze, M. C., and J. A. Francis (2006), The Arctic amplification debate, *Clim. Change*, *76*, 241–264.
- Shimada, K., T. Kamoshida, M. Itoh, S. Nishino, E. Carmack, F. McLaughlin, S. Zimmermann, and A. Proshutinsky (2006), Pacific Ocean inflow: Influence on catastrophic reduction of sea ice cover in the Arctic Ocean, *Geophys. Res. Lett.*, *33*, L08605, doi:10.1029/2005GL025624.
- Stroeve, J., M. M. Holland, W. Meier, T. Scambos, and M. Serreze (2007), Arctic sea ice decline: Faster than forecast, *Geophys. Res. Lett.*, *34*, L09501, doi:10.1029/2007GL029703.
- Winton, M. (2006), Does the Arctic sea ice have a tipping point?, *Geophys. Res. Lett.*, *33*, L23504, doi:10.1029/2006GL028017.
- Zhang, X., and J. E. Walsh (2006), Toward a seasonally ice-covered Arctic Ocean: Scenarios from the IPCC AR4 model simulations, *J. Clim.*, *19*, 1730–1747.
- 
- J. E. Overland, Pacific Marine Environmental Laboratory, NOAA, Bin C15700, 7600 Sand Point Way NE, Seattle, WA 98115, USA. (james.e.overland@noaa.gov)
- M. Wang, Joint Institute for the Study of the Atmosphere and Ocean, University of Washington, Seattle, WA 98115, USA.